Effect of Phase Separation on Spherulitic Growth Rate of PP/EPR In-Reactor Alloys

Yi-Min Liu, Ying Li, Jun-Ting Xu, Zhi-Sheng Fu, Zhi-Qiang Fan

MOE Key Laboratory of Macromolecular Synthesis and Functionalization, Department of Polymer Science & Engineering, Zhejiang University, Hangzhou 310027, China

Received 14 December 2010; accepted 12 March 2011
DOI 10.1002/app.34478
Published online 28 July 2011 in Wiley Online Library (wileyonlinelibrary.com).

ABSTRACT: In this work, the effect of phase separation on the spherulitic growth rate of a polypropylene/ethylene–propylene random (PP/EPR) copolymer in-reactor alloy was investigated. The PP/EPR in-reactor alloy was either directly quenched from homogeneous melt to crystallization temperature or held at various temperatures for phase separation prior to crystallization. It is found that at lower crystallization temperatures previous phase separation in the melt retards the crystallization rate. The higher the phase separation rate, the smaller the spherulitic growth rate. This can be attributed to faster crystallization rate than the rate of secondary phase separation. The composition of the PP-rich phase and corresponding depression of the equilibrium melting temperature of PP vary with phase separation temperature. On the other hand, at higher crystallization temperature, previous phase separation in the melt has little effect on the spherulitic growth rate because secondary phase separation can take place prior to crystallization. The transition temperature from regime II to regime III also shifts to lower temperature as the phase separation temperature increases. © 2011 Wiley Periodicals, Inc. J Appl Polym Sci 123: 535–542, 2012

Key words: phase separation; crystallization; polypropylene; in-react alloy

INTRODUCTION

Polypropylene/ethylene–propylene random copolymer (PP/EPR) in-reactor alloys have excellent mechanical properties, especially low temperature impact-resistant property.[1] The PP/EPR in-reactor alloys are usually produced by two-stage polymerization process: first, propylene homopolymerization followed by ethylene–propylene copolymerization.[2,3] The PP/EPR in-reactor alloys have a complicated microstructure and in fact are a mixture containing crystalline components: PP homopolymer, EPR copolymer, ethylene–propylene multi-block copolymer and sometimes polyethylene.[4–10]

It has been realized that in the blends containing a crystalline component the interplay of phase separation and crystallization plays an important role in morphology formation and mechanical properties of the blends.[11–19] It is found that phase separation can affect the initial stage of crystallization. For example, concentration fluctuation during phase separation may facilitate the nucleation of crystallization.[20–22] Moreover, the final morphology after crystallization is dependent on relative rates of phase separation and crystallization as well as the relative sizes of phase-separated domains and spherulites.[23–25] Recently, the concept of phase separation-crystallization interplay was introduced into PP in-reactor alloys to control the morphology and crystallization process by Han et al.[26,27] They observed that in a PP/poly(ethylene-*co*-octene) (PEOc) in-reactor alloy phase separation in the melt prior to crystallization was favorable to formation of fibril structure connecting the adjacent spherulites and inclusion of the amorphous components into the spherulites.[26] Also, they found that the nucleation rate was accelerated by phase separation.[27] However, this in-reactor alloy is prepared by dual catalysts in two reactors and it contains only two components: PP and PEOc. In the more complicated PP/EPR in-reactor alloys, we observed that phase separation had an effect on morphology similar to that in PP/PEOc, and such an effect was also dependent on the microstructure and polymerization process.[28]

The objective of this work is to study the effect of phase separation on the spherulitic growth rate of PP/EPR in-reactor alloy. So far, although there are some studies on spherulitic growth rate of PP in-reactor alloys,[29,30] the effect of phase separation on

Correspondence to: J.-T. Xu (xujt@zju.edu.cn).
Contract grant sponsor: National Natural Science Foundation of China; contract grant number: 51073138.
Contract grant sponsor: National Basic Research Program of China (973 Program); contract grant number: 2011CB606005.
Contract grant sponsor: State Key Laboratory of Chemical Engineering; contract grant number: SKL-ChE-10D04.

TABLE I
Polymerization Process and Mechanical Properties of PP/EPR In-reactor Alloy

Retention time in each polymerization cycle (min)				
Propylene homopolymerization	Ethylene-propylene copolymerization	Switch number (times)	Impact strength (kJ/m^2)	Flexural modulus (MPa)
7.5	2.5	8	13.6	915.7

the spherulitic growth is seldom considered. On the other hand, before impingement of spherulites, neither the primary nucleation process nor the secondary crystallization needs to be considered, and thus the factors affecting crystallization are simplified, and the explanation of the result becomes easier to some extent. This simplification is extremely important for the PP/EPR in-reactor alloy, which has a complicated microstructure.

EXPERIMENTAL

Preparation of PP/EPR in-reactor alloy

Details for preparation of PP/EPR in-reactor alloys were described in reference.[31] A multi-stage sequential polymerization process was conducted using a high yield spherical Ziegler-Natta catalyst, $TiCl_4$/$MgCl_2$·ID (where ID is an internal donor), kindly donated by BRICI, SINOPEC (Beijing, China). In the first stage, propylene homopolymerization was carried out for 60 min after the prepolymerization conducted in a well-stirred glass reactor. Next is a circular reaction mode including ethylene–propylene copolymerization, in which an ethylene–propylene mixture of a constant composition (propylene/ethylene = 1.5) was continuously supplied to the autoclave under constant pressure (0.4 MPa), and propylene homopolymerization under constant pressure (0.6 MPa). That is to say, after ethylene–propylene copolymerization for a designed time, the polymerization was switched to propylene homopolymerization and subsequently ethylene-propylene copolymerization at the same conditions as above. The circular reaction mode was carried out for 80 min at 60°C. The sample was synthesized by ethylene–propylene copolymerization for 2.5 min and then propylene homopolymerization for 7.5 min in a circle and its switch times was 8. The polymerization parameters and mechanical properties of this sample are given in Table I.

Polarized optical microscopy

A polarized optical microscope (Olympus BX-5) equipped with a hot-stage and a digital camera was used to study spherulitic growth of PP/EPR in-reactor alloys at different crystallization temperatures. The samples were first heated to 230°C, held for 10 min, and then cooled to the preset crystallization temperature, T_c, at a rate of 30°C/min for isothermal crystallization. During crystallization, the growth of the spherulites was monitored as a function of time. The linear growth rate, $G = dR(t)/dt$, was calculated according to the following equation:

$$R(t) = R_0 + G(T_c)(t - t_0) \quad (1)$$

where $R(t)$ is the spherulite radius, G is the linear growth rate, T_c is the crystallization temperature, t is the time, and R_0 is the so-called offset radius, which is the radius of the spherulite at t_0, which is the time we start to measure. Noting that t_0 is not the time when temperature reaches T_c ($t = 0$). We held the sample at T_c for some time and then started to measure the size of the spherulites. In all cases, the average growth rate was determined from the slope in the plots of $R(t)$ versus t. The values of t_0 may vary with experimental runs, but this has no effect on G.

RESULTS AND DISCUSSION

Effects of phase separation temperature

First, we studied the effects of phase separation temperature (T_s) and crystallization temperature (T_c) on spherulitic linear growth rate of PP/EPR in-reactor alloys. As revealed by our previous work, the phase transition temperature is $\sim$ 182°C for the PP/EPR alloy used in this work,[28] therefore, we choose 170, 160, and 150°C as the phase separation temperatures. Figure 1 shows the variations of spherulite radius with time for the PP/EPR in-reactor alloy at T_c = 130°C and T_c = 140°C, respectively. One can see that at T_c = 130°C phase separation temperature in the melt has an evident influence on the growth of the spherulites and higher phase separation temperature leads to a slower growth rate of the spherulites [Fig. 1(a)]. In contrast, at T_c = 140°C, we notice that the spherulitic growth rates only exhibit a slight difference when previous phase separation in the melt was carried out at different temperatures [Fig. 1(b)].

Figure 2 shows the variations of spherulite radius with time for the PP/EPR in-reactor alloy at various crystallization temperatures after phase separation at 170°C for 1 h. As reported for other polymers, the higher the crystallization temperature, the smaller the spherulitic growth rate. Figure 3 summarizes the

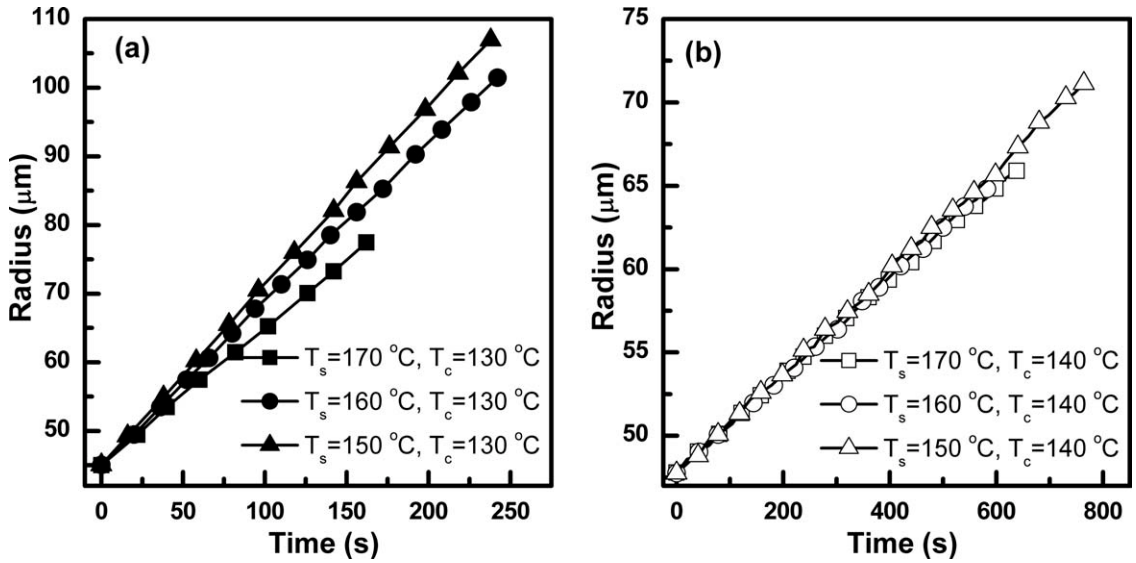

Figure 1 Variations of spherulite radius with time for the PP/EPR in-reactor alloy crystallized at $T_c = 130°C$ (a) and $T_c = 140°C$ (b) after phase separation at various temperatures for 1 h.

spherulitic growth rates at different crystallization temperatures after phase separation for 1 h at various temperatures. For comparison, the linear spherulitic growth rates of the PP/EPR in-reactor alloy directly quenched from 230°C without previous phase separation in the melt were given as well. It can be seen from Figure 3 that the linear spherulitic growth rate without previous phase separation in the melt is the largest. The linear spherulitic growth rate is retarded more severely at higher phase separation temperature. Such a phenomenon is especially evident at lower crystallization temperatures. At high crystallization temperatures, the linear spherulitic growth rates converge to the same level, irrespective of the phase separation conditions. However, since the linear spherulitic growth rates at higher crystallization temperatures are a magnitude smaller than those at lower crystallization temperatures, one may argue that the differences may be veiled when the data at lower and higher crystallization temperatures are plotted together. To clarify this argument, we used the linear spherulitic growth rates without previous phase separation in the melt as the reference, and the relative linear spherulitic

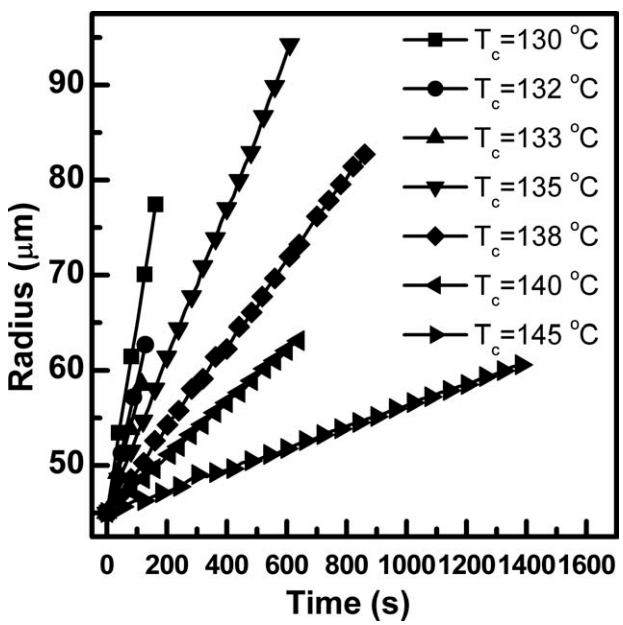

Figure 2 Variations of spherulite radius with time for PP/EPR in-reactor alloy at various crystallization temperatures after phase separation at 170°C for 1 h.

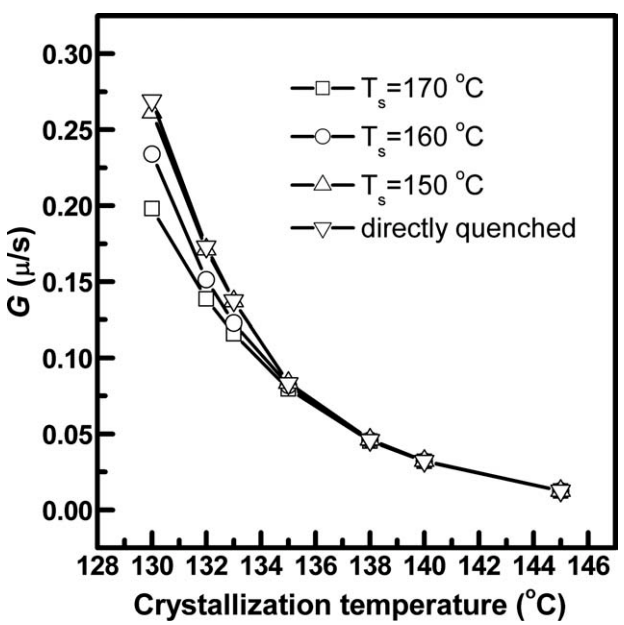

Figure 3 Linear spherulitic growth rates of PP/EPR in-reactor alloy at different crystallization temperatures after phase separation at various temperatures for 1 h.

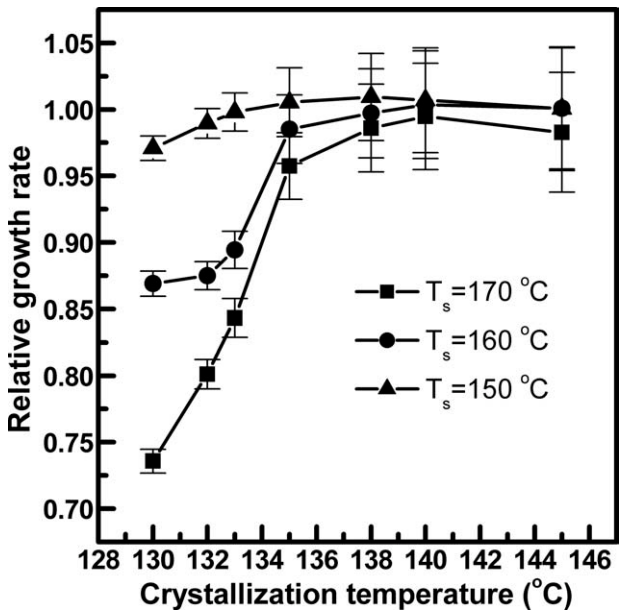

Figure 4 Relative spherulitic growth rates of PP/EPR in-reactor alloy at different crystallization temperatures after phase separation at various temperatures for 1 h.

growth rate (defined as the ratio of the G values with phase separation in the melt over that without phase separation at the same crystallization temperature) was plotted against crystallization temperature, as shown in Figure 4. It can be seen from Figure 4 that phase separation temperature indeed has an evident influence on the linear spherulitic growth rate at lower crystallization temperatures. At higher crystallization temperatures, the relative linear spherulitic growth rates at different phase separation temperatures approach to unity, though the relative errors are quite large. This means that the linear spherulitic growth rates tend to be the same at higher T_c, irrespective of the phase separation temperature in the melt. The same experiments were performed on another PP/EPR alloy prepared by two-stage polymerization process and similar results were obtained. Control experiments were also carried out for the neat PP sample. The neat PP was held at 230, 210, 190, and 170°C for 1 h, respectively, and then quenched to 132°C for crystallization. It is observed that thermal treatment in the melt at various temperatures has no obvious effect on the linear spherulitic growth rate of the neat PP. This further verifies that the effect of thermal treatment on G of the PP/EPR in-reactor alloys can be attributed to phase separation.

The effects of phase separation temperature and crystallization temperature on linear spherulitic growth rate of PP/EPR in-reactor alloy can be interpreted in terms of the phase diagram. As reported in our previous work, the PP/EPR in-reactor alloy used in the present work has an upper critical solution temperature type of phase diagram.[28] When cooled from 230°C to the selected temperatures in this work, phase separation will take place and a PP-rich phase (denoted as concentrated phase, i.e., c phase) and an EPR-rich phase (denoted as dilute phase, i.e., d phase), will be formed, as shown in Figure 5. We observed that spherulites are formed by the PP-rich phase. Although the PP in the EPR-rich phase may also crystallize, it occurs inside the formed spherulites, leading to the coarse structure of the spherulites.[28] As a result, the linear spherulitic growth rate is mainly determined by the composition of the PP-rich phase. When the phase-separated melt is further cooled to the crystallization temperature, the already present two phases may undergo new phase separation again and we called this process "secondary phase separation." The effect of phase separation on the linear spherulitic growth rate strongly depends on the relative rates of crystallization and phase separation. At higher crystallization temperatures, because phase separation is faster than crystallization, secondary phase separation will take place prior to crystallization, therefore the compositions of the PP-rich phases cooled from different phase-separated melts are the same as long as the crystallization temperature is the same. This is the reason why previous phase separation temperature in the melt has little effect on the linear spherulitic growth rate at higher crystallization temperatures. In contrast, crystallization rate overwhelms phase separation rate at lower crystallization temperature. The shallower quench depth and the confinement of the previously formed phase-separated morphology may further retard the secondary phase separation. In such a situation, the PP-rich phase starts

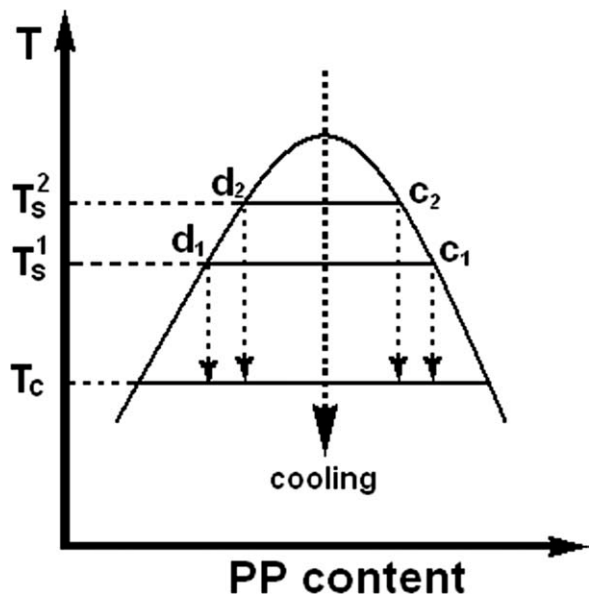

Figure 5 Schematic phase diagram for the PP/EPR in-reactor alloy.

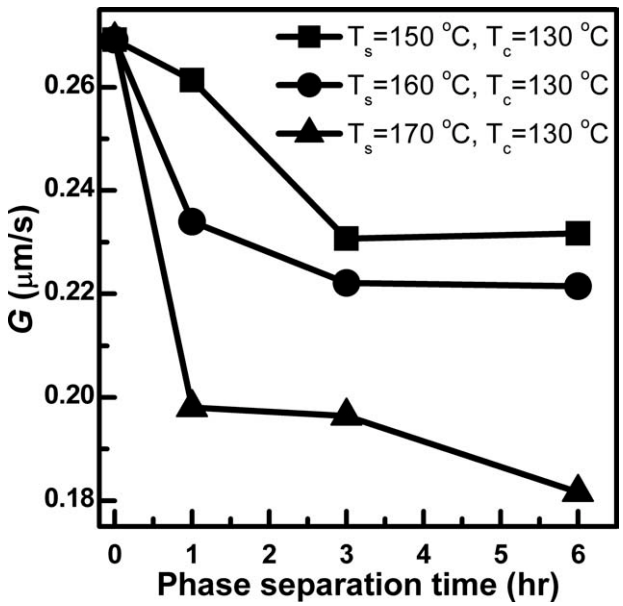

Figure 6 Effect of phase separation time in the melt on linear spherulitic growth rates of PP/EPR in-reactor alloy at $T_c = 130°C$.

crystallization from the composition at the phase separation temperature, instead of the composition at the crystallization temperature. As shown in Figure 5, the PP contents in the PP-rich phase are c_1 and c_2 at the lower phase separation temperature (T_s^1) and the higher phase separation temperature (T_s^2), respectively. Based on the phase diagram, we know c_1 is larger than c_2. When the melts with pre-phase separation at T_s^1 and T_s^2 were cooled to the same but very low crystallization temperature, the starting compositions for crystallization of the PP-rich phase are accordingly c_1 and c_2, respectively. As is well known, the miscible amorphous component can depress the melting temperature of the crystalline component.[32] As a result, even though the crystallization temperature is the same, the supercooling degrees of crystallization (defined as the difference between the equilibrium melting temperature and the crystallization temperature) are different for the PP-rich phases with different PP contents. Because crystallization rate of polymers are strongly dependent on the supercooling degree, which is apparently reflected by the dependence of crystallization rate on crystallization temperature in neat crystalline polymers. The higher the content of the amorphous component in the blend, the larger the depression of the equilibrium melting temperature and the smaller the supercooling degree at the same crystallization temperature. Because a smaller supercooling degree leads to a slower crystallization rate, the higher phase separation temperature in the melt has a stronger retardance effect on the spherulitic growth at lower crystallization temperatures.

Effect of phase separation time

We also studied the effect of phase separation time (t_s) in the melt on the linear spherulitic growth rate of the PP/EPR in-reactor alloy. As shown in Figure 6, it is found that at $T_s = 150°C$ and $T_s = 160°C$ the linear spherulitic growth rate of the PP/EPR in-reactor alloy decreases with increasing in phase separation time and becomes constant when the phase separation time is longer than 3 h. Such a phenomenon can be explained from the viewpoint of phase separation degree with time. At shorter phase separation time, the degree of phase separation is not complete. When the PP/EPR in-reactor alloy is cooled to crystallization temperature, the driving force for secondary phase separation is still strong and the difference due to the different phase separation temperatures may be weakened. We notice that there is still a weak tendency of decrease in the linear spherulitic growth rate at $T_s = 170°C$ when the phase separation time is beyond 3 h. This is possibly due to the slower phase separation rate at $T_s = 170°C$ arising from the shallower quench depth in temperature. It should be noted that the effect of the previous phase separation in the melt also depends on the microstructure and phase transition temperature of the PP/EPR in-reactor alloy. Shangguan et al. observed that the thermal treatment at 200°C for different times has little effect on linear spherulitic growth rate of another PP/EPR in-reactor alloy.[29,30]

Shift of crystallization regimes

The crystallization temperature of polymer can usually be classified into three regimes based on Lauritzen-Hoffman's theory.[33,34] In regime I, the secondary nucleation rate (i) is far less than the growth rate of polymer crystals (g) on the lateral surface, and in regime II the value of i is comparable with that of g. When crystallization occurs in regime III, the secondary nucleation rate becomes larger than the growth rate of polymer crystals on the lateral surface.

The Lauritzen-Hoffman's theory can be expressed as:

$$G = G_0 \exp[-U^*/R(T_c - T_0)] \exp[-K_g/T_c(\Delta T)f] \quad (2)$$

where G is the linear spherulitic growth rate, T_c is the crystallization temperature, G_0 is a constant and is independent of temperature, U^* is the activation energy related with the short distance diffusion of the crystalline unit across the phase boundary, K_g is the nucleation constant, T_0 is the temperature below which there is no chain motion (usually $T_0 = T_g - 30$ K), ΔT is the supercooling ($\Delta T = T_m^0 - T_c$), i.e., the difference between the equilibrium melting temperature (T_m^0) and the crystallization temperature

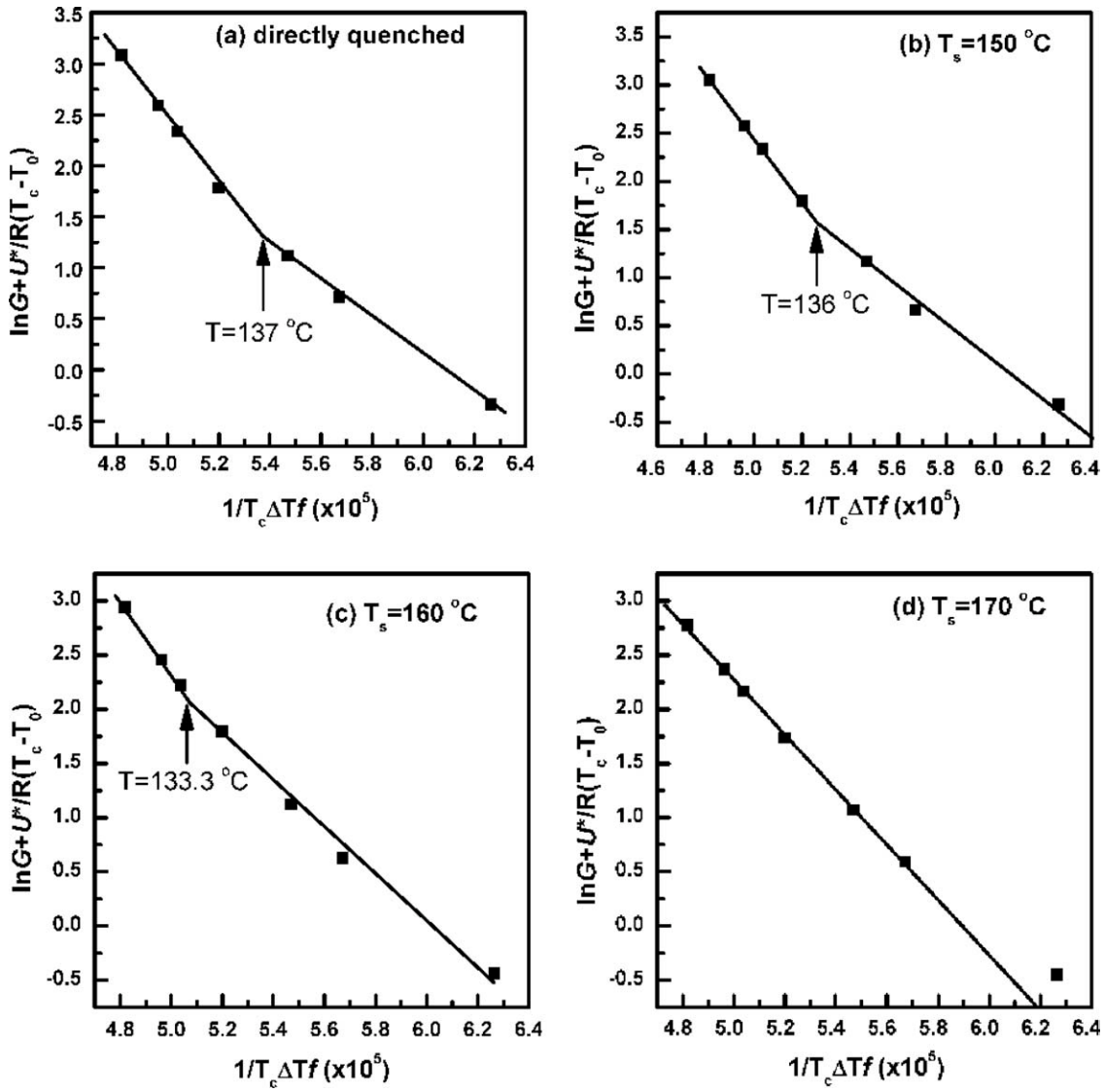

Figure 7 Plots of $\ln G + U^*/R(T_c - T_0)$ versus $1/T_c(\Delta T)f$ for the PP/EPR in-reactor alloy. (a) Directly quenched from 230°C; (b) $T_s = 150$°C; (c) $T_s = 160$°C; (d) $T_s = 170$°C.

(T_c), f is the correction factor and is equal to $2T_c/(T_m^0 + T_c)$. Equation (2) can be reformed into:

$$\ln G + U^*/R(T_c - T_0) = \ln G_0 - K_g/T_c(\Delta T)f \quad (3)$$

As a result, the nucleation constant, K_g, can be obtained from the slope in the plot of $\ln G + U^*/R(T_c - T_0)$ versus $1/T_c(\Delta T)f$.

The nucleation constant, K_g, can also be expressed as[35]:

$$K_g = jb_0\sigma\sigma_e T_m^0/k(\Delta h_f) \quad (4)$$

where $j = 4$ for crystallization regimes I and III, and $j = 2$ for crystallization regime II, b_0 is the layer thickness, σ_e is the fold surface free energy, σ is the lateral surface free energy, Δh_f is fusion enthalpy and k is Boltzmann's constant.

For crystallization of miscible polymer blends, modified Lauritzen-Hoffman model was proposed[36–38]:

$$\ln G - \ln \varphi_2 + U^*/R(T_c - T_0) - 0.2T_m^0 \ln \varphi_2 = \ln G_0 - K_g/T_c(\Delta T)f \quad (5)$$

where φ_2 is the volume fraction of the crystalline component in the blends.

It should be emphasized that eq. (5) is only applicable to the totally miscible blends without phase separation. Two difficulties are encountered when eq. (5) is applied to the present PP/EPR in-reactor alloy: (1) We have no the exact phase diagram of the PP/EPR in-reactor alloy due to its complicated microstructure and the compositions in the concentrated and dilute phases are unknown. (2) The compositions of the concentrated and dilute phases may changes with phase separation temperature and

crystallization temperature. As a result, we still use eq. (3) to process the data of linear spherulitic growth rate in the present work. The values of U^*, T_m^0, T_0, Δh_f, b_0, and σ are 6.28 kJ/mol, 458.2 K, 231.2 K, 1.96×10^8 J/m^3, 6.26 Å, and 11.5 erg/cm^2, respectively.[33,35,39,40]

Figure 7 shows the plots of $\ln G + U^*/R(T_c - T_0)$ versus $1/T_c(\Delta T)f$ for the PP/EPR in-reactor alloy crystallized from directly quenched melt and from previous phase-separated melts at various T_s. The data in Figure 7(a) show that the transition temperature from crystallization regime II to regime III ($T_{II \to III}$) for the sample directly quenched from 230°C is 137°C. When phase separation was carried out in the melt prior to crystallization, $T_{II \to III}$ decreases gradually as the phase separation temperature increases, the values of $T_{II \to III}$ are 136°C and 133.3°C for $T_s = 150$°C and $T_s = 160$°C, respectively. For $T_s = 170$°C, no transition from regime II to regime III is observed in the range of crystallization temperature studied, which indicates that $T_{II \to III}$ is smaller than 130°C. Apparently, we can see that previous phase separation in the melt affects the transition temperature from regime II to regime III. The shift of $T_{II \to III}$ to lower temperature (compared with the neat PP) was also observed for PP blends[41] as well as PP in-reactor alloys.[29,30]

There are two possible reasons for the shift of $T_{II \to III}$. The first is the dependence of the supercooling on the composition. As shown in the schematic phase diagram (Fig. 5), the PP-rich phase has a lower PP content at higher T_s, resulting in a larger supercooling degree at the same crystallization temperature. The means that, at a given crystallization temperature, it is in regime III for the PP/EPR alloy with previous phase separation at lower T_s due to a larger supercooling degree, but it may be in regime II for the PP/EPR alloy with previous phase separation at higher T_s due to a smaller supercooling degree. This shows the supercooling degree, which varies with the phase separation temperature in the melt, further affects the transition temperature from crystallization regime II to regime III. On the other hand, the composition of the PP-rich phase may also affect the secondary nucleation rate and the free energy of the lateral surface, leading to the shift of $T_{II \to III}$.

CONCLUSIONS

The earlier results show that when crystallization occurs at lower temperature, crystallization rate is faster than the rate of secondary phase separation. As a result, the composition of the preformed PP-rich phase has an effect on the equilibrium melting temperature and supercooling, leading to decrease of the spherulitic growth rate with phase separation temperature. The retardance effect of phase separation becomes stronger as phase separation time increases and then reaches a constant level. However, at high crystallization temperature, the crystallization rate is slower than the rate of secondary phase separation. Therefore, secondary phase separation can take place prior to crystallization and the previous phase separation in the melt has little effect on the spherulitic growth rate. As phase separation temperature increases, the transition temperature from crystallization regime II to regime III shifts to lower temperature.

References

1. Galli, P.; Haylock, J. C. Prog Polym Sci 1991, 16, 443.
2. Simonazzi, T.; Cecchin, G.; Mazzullo, S. Prog Polym Sci 1991, 16, 303.
3. Galli, P.; Vecellio, G. Prog Polym Sci 2001, 26, 1287.
4. Mirabella, F. M. J Polymer 1993, 34, 1729.
5. Cai, H. J.; Luo, X. L.; Ma, D. Z.; Wang, J. M.; Tan, H. S. J Appl Polym Sci 1999, 71, 93.
6. Fu, Z. S.; Fan, Z. Q.; Zhang, Y. Z.; Xu, J. T. Polym Int 2004, 53, 1169.
7. Xu, J. T.; Feng, L. X. Polym Int 1998, 47, 433.
8. Fan, Z. Q.; Zhang, Y. Q.; Xu, J. T.; Wang, H. T.; Feng, L. X. Polymer 2001, 42, 5559.
9. Fu, Z. S.; Xu, J. T.; Zhang, Y. Z.; Fan, Z. Q. J Appl Polym Sci 2005, 97, 640.
10. de Goede, E.; Mallon, P.; Pasch, H. Macromol Mater Eng 2010, 295, 366.
11. Tanaka, H.; Nishi, T. Phys Rev Lett 1985, 55, 1102.
12. Tanaka, H.; Nishi, T. Phys Rev A 1989, 39, 783.
13. Crist, B.; Hill, M. J. J Polym Sci Part B: Polym Phys 1997, 35, 2329.
14. Lim, S. W.; Lee, K. H.; Lee, C. H. Polymer 1999, 40, 2837.
15. Wang, H.; Shimizu, K.; Hobbie, E. K.; Wang, Z. G.; Meredith, J. C.; Karim, A.; Amis, E. J.; Hsiao, B. S.; Hsieh, E. T.; Han, C. C. Macromolecules 2002, 35, 1072.
16. Shimizu, K.; Wang, H.; Wang, Z. G.; Matsuba, G.; Kim, H.; Han, C. C. Polymer 2004, 45, 7061.
17. Wang, Z. G.; Wang, H.; Shimizu, K.; Dong, J. Y.; Hsiao, B. S.; Han, C. C. Polymer 2005, 46, 2675.
18. Niu, Y. H.; Wang, Z. G.; Orta, C. A.; Xu, D. H.; Wang, H.; Shimizu, K.; Hsiao, B. S.; Han, C. C. Polymer 2007, 48, 6668.
19. Shimizu, K.; Wang, H.; Matsuba, G.; Wang, Z. G.; Kim, H.; Peng, W. Q.; Han, C. C. Polymer 2007, 48, 4226.
20. Zhang, X. H.; Wang, Z. G.; Muthukumar, M.; Han, C. C. Macromol Rapid Commun 2005, 26, 1285.
21. Zhang, X. H.; Wang, Z. G.; Dong, X.; Wang, D. J.; Han, C. C. J Chem Phys 2006, 125, 024907.
22. Zhang, X. H.; Man, X. K.; Han, C. C.; Yan, D. D. Polymer 2008, 49, 2368.
23. Wang, H.; Shimizu, K.; Kim, H.; Hobbie, E. K.; Wang, Z. G.; Han, C. C. J Chem Phys 2002, 116, 7311.
24. Inaba, N.; Sato, K.; Suzuki, S.; Hashimoto, T. Macromolecules 1986, 19, 1690.
25. Inaba, N.; Yamada, T.; Suzuki, S.; Hashimoto, T. Macromolecules 1988, 21, 407.
26. Du, J.; Niu, H.; Dong, J. Y.; Dong, X.; Wang, D.; He, A.; Han, C. C. Macromolecules 2008, 41, 1421.
27. Du, J.; Zhang, X. H.; Han, C. C. J Polym Sci Part B: Polym Phys 2009, 47, 166.
28. Li, Y.; Xu, J. T.; Dong, Q.; Fu, Z. S.; Fan, Z. Q. Polymer 2009, 50, 5134.

29. Xu, J. T.; Fu, Z. S.; Wang, X. P.; Geng, J. S.; Fan, Z. Q. J Appl Polym Sci 2005, 98, 632.
30. Shangguan, Y. G.; Song, Y. H.; Zheng, Q. Polymer 2007, 48, 4567.
31. Dong, Q.; Wang, X. F.; Fu, Z. S.; Xu, J. T.; Fan, Z. Q. Polymer 2007, 48, 5905.
32. Nishi, T.; Wang, T. T. Macromolecules 1975, 8, 909.
33. Lauritzen, J. I.; Hoffman, J. D. J Appl Phys 1973, 44, 4340.
34. Hoffman, J. D.; Davis, G. T.; Lauritzen, J. I. In Chemistry Crystallization and Noncrystalline Solid. Hannay, N. B., ed. Vol. 3. Plenum Press: New York, 1976.
35. Clark, E. J.; Hoffman, J. D. Macromolecules 1984, 17, 878.
36. Alfonso, G. C.; Russell, T. P. Macromolecules 1986, 19, 1143.
37. Martuscelli, E. Polym Eng Sci 1984, 24, 563.
38. Boon, J.; Azcue, J. M. J Polym Sci Part A-2: Polym Phys 1968, 6, 885.
39. Cheng, S. Z. D.; Janimak, J. J.; Zhang, A.; Cheng, H. N. Macromolecules 1990, 23, 298.
40. Hoffman, J. D.; Miller, R. L.; Marand, H.; Roitman, D. B. Macromolecules 1992, 25, 2221.
41. Yamaguchi, M.; Miyata, H.; Nitta, K. H. J Polym Sci Part B: Polym Phys 1997, 35, 953.